

Supporting Information

Self-immobilization of coacervate droplets by enzyme-mediated hydrogelation

Yufeng Chen,^a Yanwen Zhang,^a Mei Li,^b Songyang Liu,^a Xiaohai Yang,^a Kemin Wang,^a Stephen Mann,^{*b} and Jianbo Liu^{*a}

-
- a. State Key Laboratory of Chemo/Biosensing and Chemometrics, College of Chemistry and Chemical Engineering, Key Laboratory for Bio-Nanotechnology and Molecular Engineering of Hunan Province, Hunan University, Changsha 410082, P. R. China. Email: liujianbo@hnu.edu.cn.
- b. Centre for Protolife Research, Max Planck-Bristol Centre for Minimal Biology, School of Chemistry, University of Bristol, Bristol BS8 1TS, UK; School of Materials Science and Engineering, Shanghai Jiao Tong University, Shanghai 200240, P. R. China. Email: s.mann@bristol.ac.uk.

Table of Contents

Experiment section

Table S1. Change of position in the 3D reconstruction of coacervate microdroplets.

Figure S1. Zeta potentials of coacervate microdroplets.

Figure S2. Bright imaging (A) and fluorescence images (B) of coacervate microdroplets.

Figure S3. Time profiles of resorufin production (changes in fluorescence intensity) in GOx/HRP-containing coacervate microdroplets at various glucose concentrations.

Figure S4. ABTS catalyzed by GOx in PBS buffer and GOx loaded in coacervate microdroplets with different amounts of glucose by UV-Vis spectra.

Figure S5. Michaelis–Menten kinetic fitting of GOx activity in PBS buffer and in a coacervate suspension.

Figure S6. Amplex red catalyzed by GOx loaded in coacervate microdroplets with different amounts of glucose by CLSM.

Figure S7. Percentage transmittance of DEAE-dextran/DNA coacervates at pH values of 7.4 and 3.5. The similar values of transmission indicate that the coacervate phase is retained at acidic pH.

Figure S8. Enzyme-mediated pH change in coacervate microdroplets prepared at different weight ratios.

Figure S9. The standard curve of Fura-2 with different concentration of Ca²⁺.

Figure S10. ICP-AES quantitative analysis of Ca²⁺.

Figure S11. The effect of coacervate density on the hydrogelation.

Figure S12. Rheometry dynamic strain sweeps of alginate-Ca²⁺ hydrogel.

Figure S13. FTIR spectra of calcium alginate and sodium alginate.

Figure S14. Frozen section of calcium alginate hydrogel loaded with different concentrations of coacervates.

Figure S15. 3D image of calcium alginate hydrogels loaded with different concentrations of coacervates.

Figure S16. Optical images of coacervate microdroplets suspension with different amounts of NaCl.

Figure S17. Optical images of coacervate microdroplets in alginate-Ca²⁺ hydrogel with different amounts of NaCl.

Experimental Section

Materials: Deoxyribonucleic acid (DNA, low molecular weight from salmon sperm), DEAE-Dextran hydrochloride (500 kDa), Fura-2 penta-potassium salt, glucose, CaCO₃ (98%), glucose oxidase (GOx), Amplex red and Hoechst 33258, horseradish peroxidase (HRP), were purchased from Sigma-Aldrich. Sodium alginate (low viscosity) was purchased from J&K Scientific. 2,2'-Azino-bis (3-ethylbenzthiazoline-6-sulfonic acid) (ABTS) and deoxyribonuclease I (DNase I) were purchased from Sangon Biotech. Milli-Q-purified water (18.2 MΩ·cm) was used for all the experiments.

Instrumentation: The Fourier-transform infrared spectra (FTIR) were recorded on Bruker Tensor 27 at room temperature. The KBr disk method was adopted for the experiment, and samples were scanned over the range of 4000–400 cm⁻¹. The prototissue histological section experiment was carried out with a Leica CM1950. The thickness of the frozen hydrogel slice was 10 μm at -28 °C and was imaged by inverted fluorescence microscope (20× objective). Fluorescence confocal microscopic imaging was performed by TI-E+A1 SI, Nikon confocal laser scanning microscope with Ar laser. Three-dimensional reconstructions from Z scans were performed using Image J (plugin 3D viewer).

Preparation of DEAE-dextran/DNA coacervate microdroplets: The microdroplet dispersions were prepared by mixing of DEAE-dextran solution (10.0 mg·mL⁻¹, pH=8.0) and DNA solution (10 mg·mL⁻¹, pH=8.0) at the ratio of 2:1 (DEAE-dextran: DNA, w/w). The guest molecules, including GOx, FITC-GOx and CaCO₃ were synchronously doped and sequestered in the coacervate matrix. FITC labeling of GOx protein was prepared according to previous methods.^[1] The partition constant (K) was determined from $K = \frac{[\text{Guest object}]_{\text{in}}}{[\text{Guest object}]_{\text{out}}}$, where $[\text{Guest object}]_{\text{in}}$ was equal to $([\text{Guest object}]_{\text{total}} * V_{\text{total}} - [\text{Guest object}]_{\text{out}} * V_{\text{out}}) / V_{\text{in}}$, and $[\text{Guest object}]_{\text{out}}$ and V_{out} , and $[\text{Guest object}]_{\text{in}}$ and V_{in} , were the concentrations and volumes (V) of guest object in the continuous aqueous phase and coacervate phase, respectively.^[2]

Glucose triggered dissolution of CaCO₃ and gelation of calcium alginate hydrogels: DEAE-dextran/DNA coacervate microdroplets (5 mg·mL⁻¹) loaded with GOx (0.1 mg·mL⁻¹) and CaCO₃ powder (0.4 mg·mL⁻¹) were dispersed in sodium alginate (1%, pH=8.0). Different amounts of glucose (0 - 33.0 mM) were added to the microdroplet suspension and incubated for more than 6 h, after which the coacervate microdroplets became immobilized in an alginate-Ca²⁺ hydrogel.

Amplex red fluorescence assay: DEAE-dextran/DNA coacervate microdroplets (5 mg·mL⁻¹) loaded with 0.1 mg·mL⁻¹ GOx and 4.4 μg·mL⁻¹ HRP were dispersed in 10 mM PBS solution containing 40 μM Amplex red. To start the cascade reaction, 33.0 mM glucose was added to the sample and a time series was monitored immediately by CLSM (Ex: 561 nm, Em: 585 nm). Image J software was used for data processing.

Enzymatic activity measurements: The enzymatic activity of GOx in all samples was evaluated by UV-vis spectroscopy using a H₂O₂-ABTS colorimetric assay in which a phosphate buffer solution (10 mM, pH 7.4), 4.4 μg·mL⁻¹ HRP, 0.075 μg·mL⁻¹ GOx, 0 – 750 mM glucose and 2 mM ABTS were mixed together. To determinate the enzyme activity of GOx, the time-dependent UV absorption change associated with oxidation of ABTS in the coacervate phase or in bulk aqueous solution to an ABTS-diradical (418 nm, ε₄₁₈ = 36,800 M⁻¹·cm⁻¹)^[3] was recorded.

Fluorescent measurement of calcium ions: Ca²⁺ ions were monitored using the Fura-2 penta potassium fluorescence method.^[4] Fura-2 is a ratiometric fluorescent Ca²⁺ indicator. Binding of free Ca²⁺ ions to Fura-2 changes the peak excitation wavelength from 380 to 340 nm, whereas the peak emission around 510 nm remains unchanged. Fluorescence signals at 510 nm were collected with sequential excitation at 340, 380 nm, respectively, for samples incubated with 5 μM Fura-2. Emission ratios from the 340/380 nm excitation were converted into a measurement of the free Ca²⁺ concentration using the following equation,

$$[\text{Ca}^{2+}] = K_d * \frac{F_{\text{max}}}{F_{\text{min}}} * \frac{(R - R_{\text{min}})}{(R_{\text{max}} - R)} \quad (\text{Equation S1})$$

where K_d is the dissociation constant for Fura-2 (224 nM), R is the experimental emission ratios and F_{min} , R_{max} , F_{max} and R_{min} are the fluorescence emission signals at 380 nm and emission ratio from 340/380 nm

excitation at saturating and zero free Ca^{2+} levels, respectively. In this experiment, $R_{\min} = 0.807$, $R_{\max} = 3.593$, $K_d = 224 \text{ nM}$, and $F_{\max}/F_{\min} = 2.308$.

Rheological analysis: Rheological measurements were carried out with a stress-controlled Rheometer MCR 102 (Anton Par Instruments) in a cone-plate geometry. The upper plate (20 mm diameter) was lowered until contact with the solution surface, and the examination was performed by oscillatory frequency sweeps ($0.1\text{--}100 \text{ rad}\cdot\text{s}^{-1}$, 0.5% strain). The hydrogel solutions were loaded onto the rheometer and the upper plate was lowered to a gap size of $50 \mu\text{m}$. A time sweep was performed at $20 \text{ }^\circ\text{C}$ and 0.5% strain for 6 h.

Hydrogel compression experiments: Two pieces of cover glass ($22 \times 22 \text{ mm}$) were placed on the surface of a coacervate microdroplet-containing alginate- Ca^{2+} hydrogel. The sample was then compressed at a pressure of 120 Pa and *in situ* 3D reconstruction confocal imaging used to determine the positional changes of the embedded coacervate microdroplets.”

Anti-enzymatic and anti-salt experiments: In order to compare the stability of coacervate microdroplets dispersed in aqueous alginate suspension or an alginate- Ca^{2+} hydrogel, anti-enzymatic and anti-salt experiments were conducted. NaCl ($0\text{--}1.0 \text{ M}$) or DNase I ($20 \text{ U}\cdot\text{mL}^{-1}$) were added into the coacervate microdroplet suspension ($5 \text{ mg}\cdot\text{mL}^{-1}$) dispersed in aqueous alginate or immobilized within a 1.0 % alginate- Ca^{2+} hydrogel. The coacervate morphology was determined through inverted fluorescence microscope at different time intervals.

Table S1. Changes in spatial location for coacervate microdroplets obtained from 3D reconstructions of the hydrogel-embedded microdroplets.

Numbers	1	2	3	4
Coordination/ μm (X, Y, Z)	(10.5, 41.6, 45.5)	(24.1, 35.6, 35.8)	(49.5, 43.8, 43.3)	(56.9, 49.2, 93.6)
Numbers	3'	2'	1'	4'
Coordination/ μm (X, Y, Z)	(10.8, 40.2, 26.3)	(24.8, 34.4, 20.3)	(48.7, 48.4, 25.1)	(58.2, 47.2, 60.1)

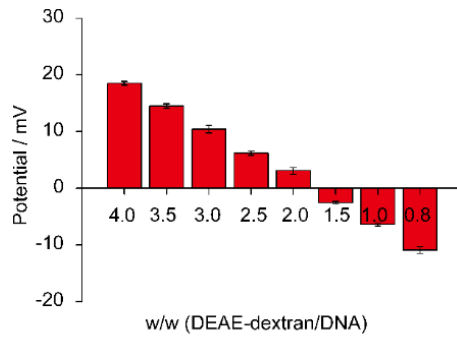


Figure S1. Plot of zeta potentials for DEAE-dextran/DNA coacervate microdroplets prepared at different DEAE-dextran ($10.0 \text{ mg}\cdot\text{mL}^{-1}$, $\text{pH}=8.0$) and DNA ($10 \text{ mg}\cdot\text{mL}^{-1}$, $\text{pH}=8.0$) weight ratios.

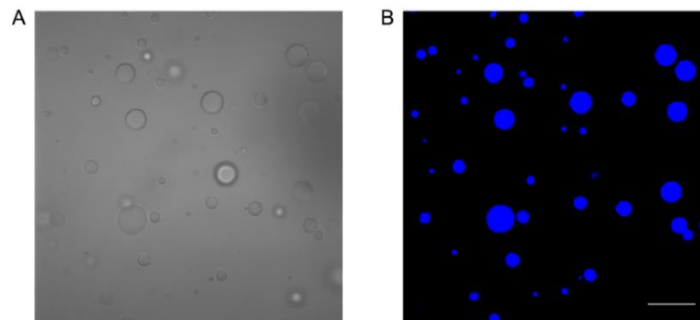


Figure S2. Bright field (A) and fluorescent field (B) images of DEAE-dextran/DNA coacervate microdroplets stained with the DNA binding dye of Hoechst 33258. Ex: 405 nm, Em: 465 nm. Scale bar: $20 \mu\text{m}$.

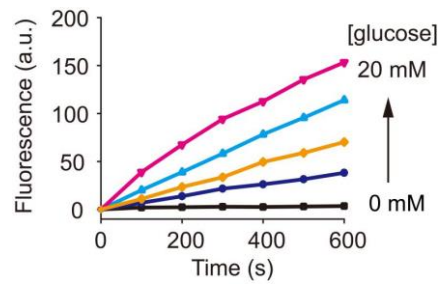


Figure S3. Time profiles of resorufin production (changes in fluorescence intensity) in GOx/HRP-containing coacervate microdroplets at various glucose concentrations (0–20 mM).

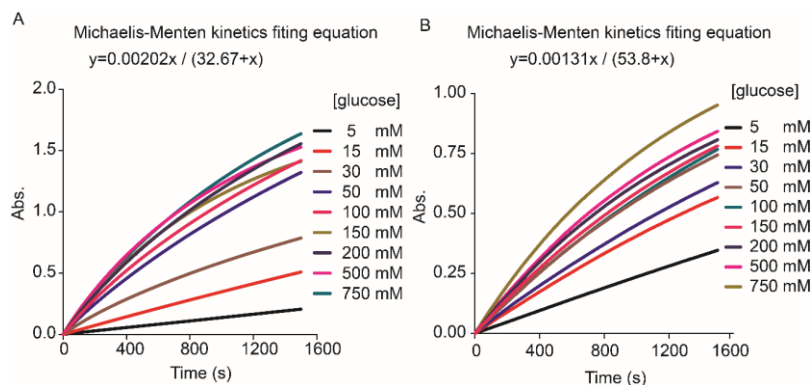


Figure S4. Time-dependent changes in ABTS absorbance (410 nm) associated with GOx ($0.075 \mu\text{g}\cdot\text{mL}^{-1}$)/HRP ($4.4 \mu\text{g}\cdot\text{mL}^{-1}$) enzyme cascades undertaken in the presence of different amounts of glucose (5–750 mM). (A) GOx/HRP in PBS buffer (10 mM, pH=7.4). (B) GOx/HRP loaded into DEAE-dextran/DNA coacervate microdroplets. Data are fitted to a Michaelis-Menten kinetic model.

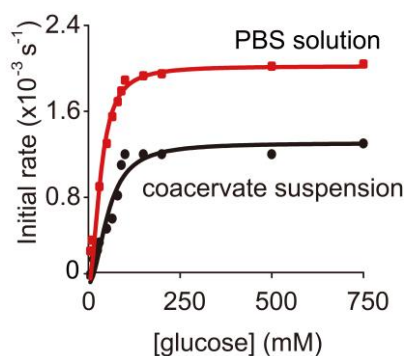


Figure S5. Michaelis–Menten kinetic fitting of GOx activity in 10 mM PBS buffer (pH 7.4) and in a coacervate hydrogel as determined using the ABTS colorimetric method (GOx, $0.075 \mu\text{g}\cdot\text{mL}^{-1}$; HRP, $4.4 \mu\text{g}\cdot\text{mL}^{-1}$; ABTS, 2 mM). The kinetic data were fitted to a Michaelis–Menten model, which gave a Michaelis constant (K_M) and turnover number (k_{cat}) of 53.80 mM and $1.27 \times 10^{-3} \text{ s}^{-1}$, respectively, which indicated that although functional, GOx exhibited a lower activity in the coacervate phase than in bulk solution ($K_M = 2.67 \text{ mM}$, $k_{\text{cat}} = 2.26 \times 10^{-3} \text{ s}^{-1}$) in agreement with previous studies.

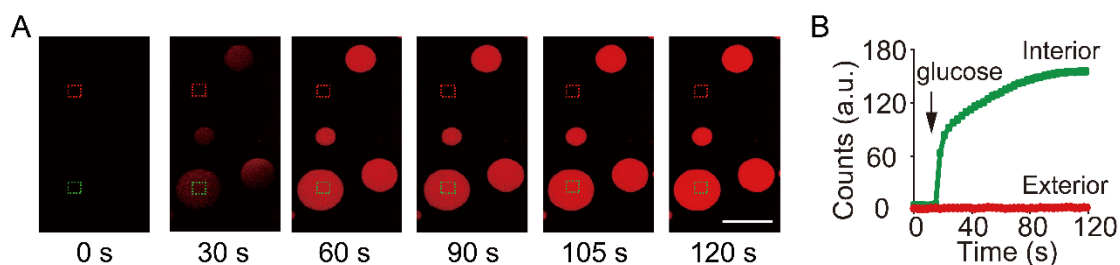


Figure S6. A) Time-dependent fluorescence confocal imaging of resorufin production (red fluorescence) within GOx/HRP-containing coacervate microdroplets after addition of glucose (33.0 mM). Scale bar: $20 \mu\text{m}$. B) Time profile of the change in fluorescence intensity in the external solution (red line) and interior (green line) of the coacervate droplet highlighted in (A).

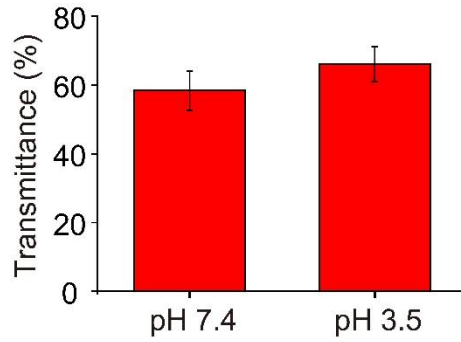


Figure S7. Percentage transmittance of DEAE-dextran/DNA coacervates at pH values of 7.4 and 3.5. The similar values of transmission indicate that the coacervate phase is retained at acidic pH.

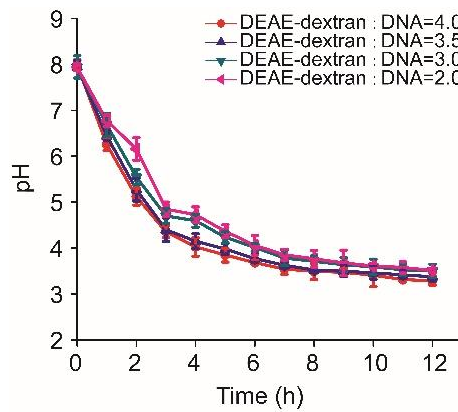


Figure S8. Enzyme-mediated pH changes in coacervate microdroplets prepared at different DEAE-dextran/DNA weight ratios. GOx: 0.1 mg mL⁻¹, glucose: 100 mM.

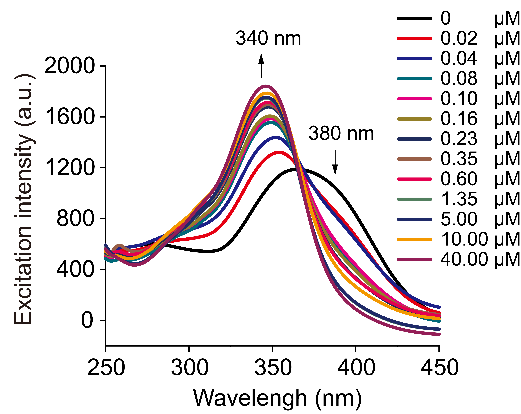


Figure S9. Fura-2 calibration curves obtained at different concentrations of Ca²⁺, Fura-2: 5 μM, Ex=340, 380 nm, respectively, Em=510 nm.

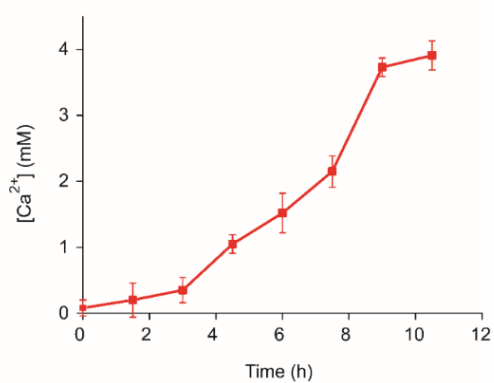


Figure S10. ICP-AES quantitative analysis of released Ca²⁺ concentration at different time intervals after addition of glucose (33.0 mM) to coacervate microdroplets (5 mg·mL⁻¹) containing CaCO₃ (0.4 mg·mL⁻¹) and GOx (0.1 mg·mL⁻¹). Data were obtained after 2500 times dilution.

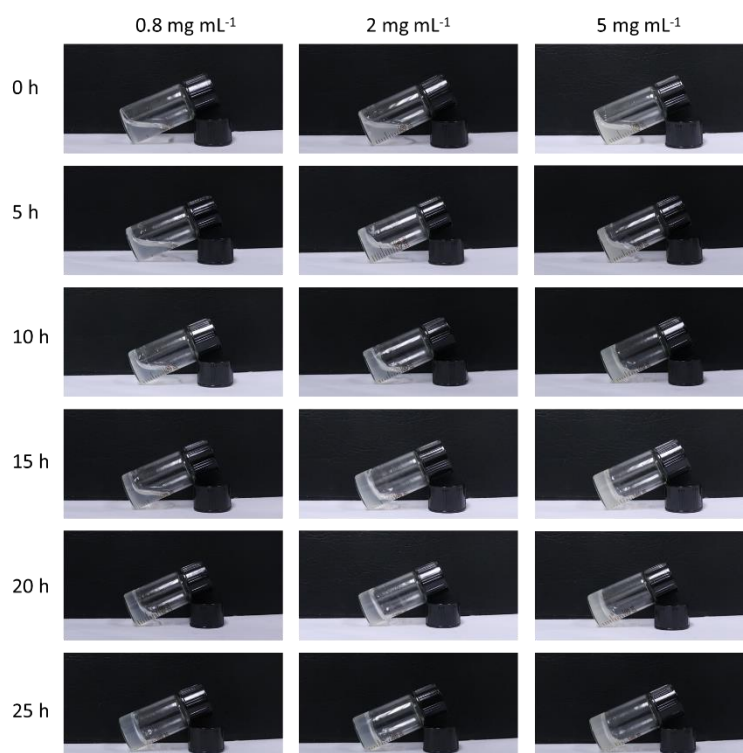


Figure S11. Effect of coacervate number density (concentrations, 0.8, 2, 5 mg mL⁻¹) on hydrogelation. GOx: 0.1 mg mL⁻¹, sodium alginate: 1%, glucose: 30 mM, CaCO₃: 0.4 mg·mL⁻¹.

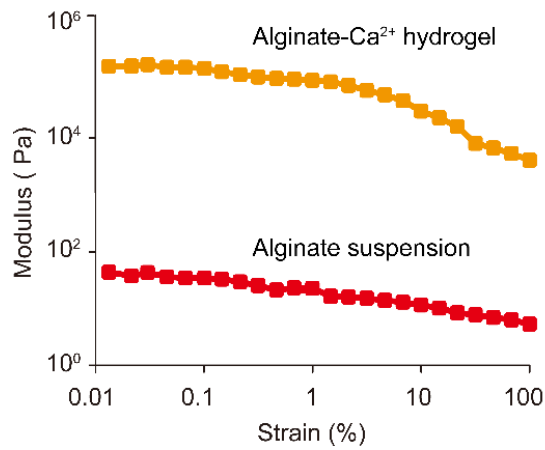


Figure S12. Rheometry dynamic strain sweeps recorded at 1 Hz frequency of the storage modulus (G') for a dispersion of GOx/ CaCO_3 -containing coacervate microdroplets in sodium alginate before and 6 h after addition of glucose (hydrogelation). Coacervate, $5 \text{ mg}\cdot\text{mL}^{-1}$; GOx, $0.1 \text{ mg}\cdot\text{mL}^{-1}$; CaCO_3 , $0.4 \text{ mg}\cdot\text{mL}^{-1}$; glucose, 33.0 mM .

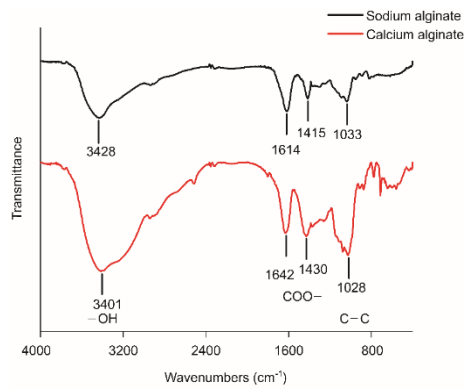


Figure S13. FTIR spectra of calcium alginate (red) and sodium alginate (1%, black) in the presence of coacervate microdroplets ($5 \text{ mg}\cdot\text{mL}^{-1}$) containing GOx and CaCO_3 particles ($0.4 \text{ mg}\cdot\text{mL}^{-1}$). The former is produced after addition of glucose. Samples were freeze-drying before FTIR characterization.

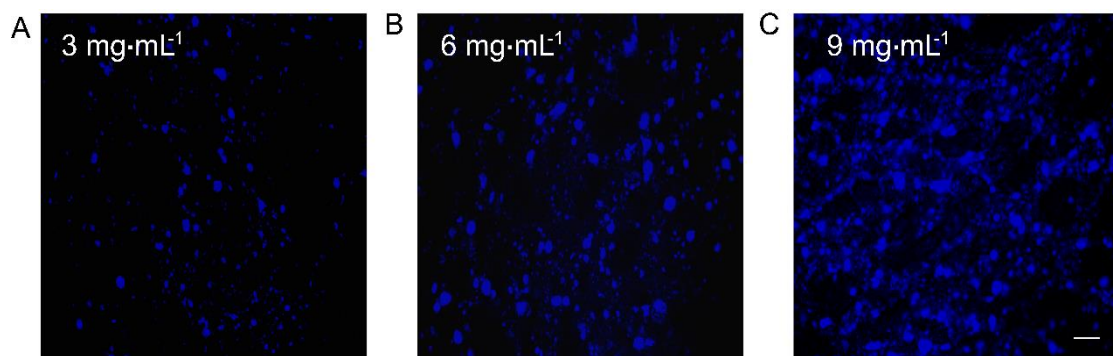


Figure S14. Frozen histological sectioned image of alginate- Ca^{2+} hydrogels prepared from different coacervate concentrations. In each case, the microdroplets are stained with Hoechst 33258 and are observed throughout the hydrogels; scale bar: $50 \mu\text{m}$.

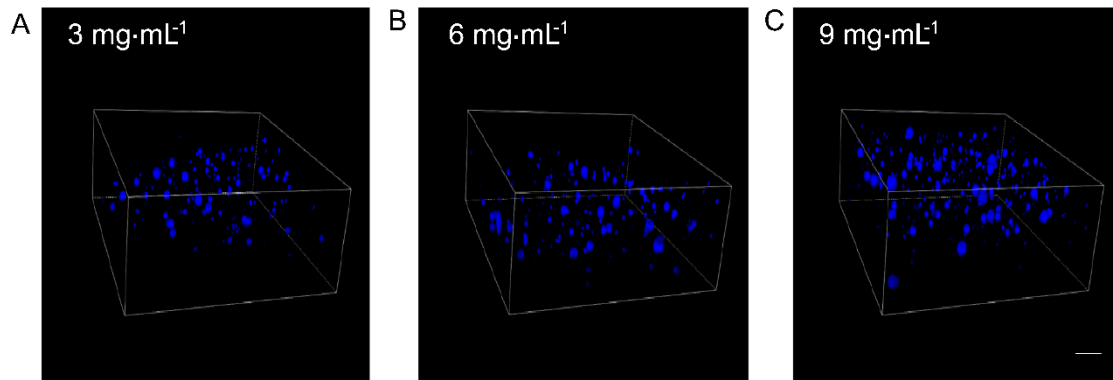


Figure S15. 3D fluorescence microscopy images of alginate- Ca^{2+} hydrogel prepared from different coacervate concentrations. In each case, the microdroplets are stained with Hoechst 33258 and are observed throughout the hydrogels; scale bar: 50 μm .

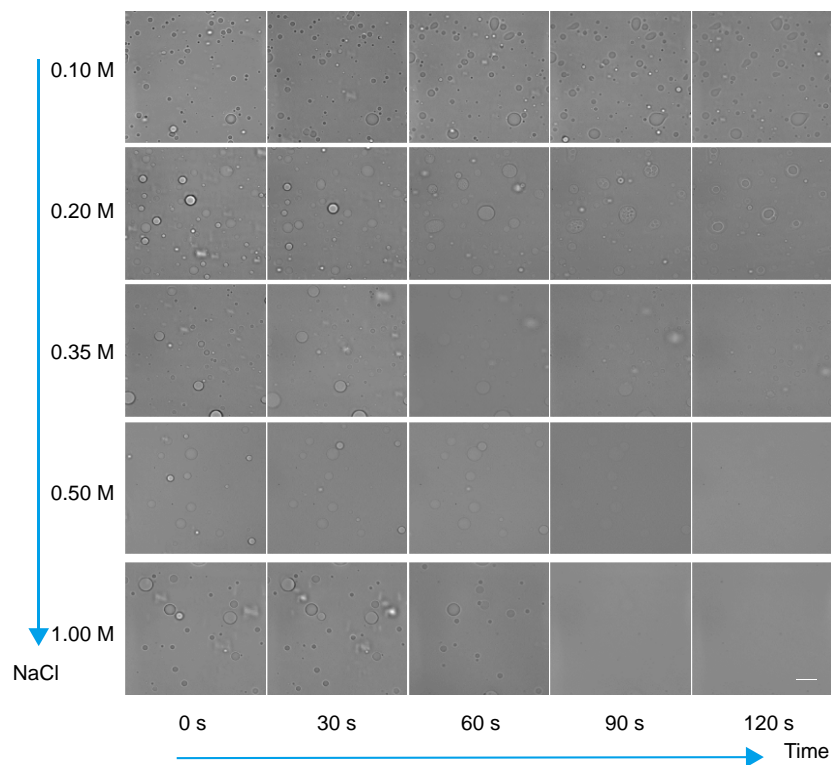


Figure S16. Time-dependent optical microscopy images of coacervate-containing alginate suspensions after addition of different amounts of NaCl (0.1, 0.2, 0.35, 0.5, 1.0 M). Scale bar: 10 μm .

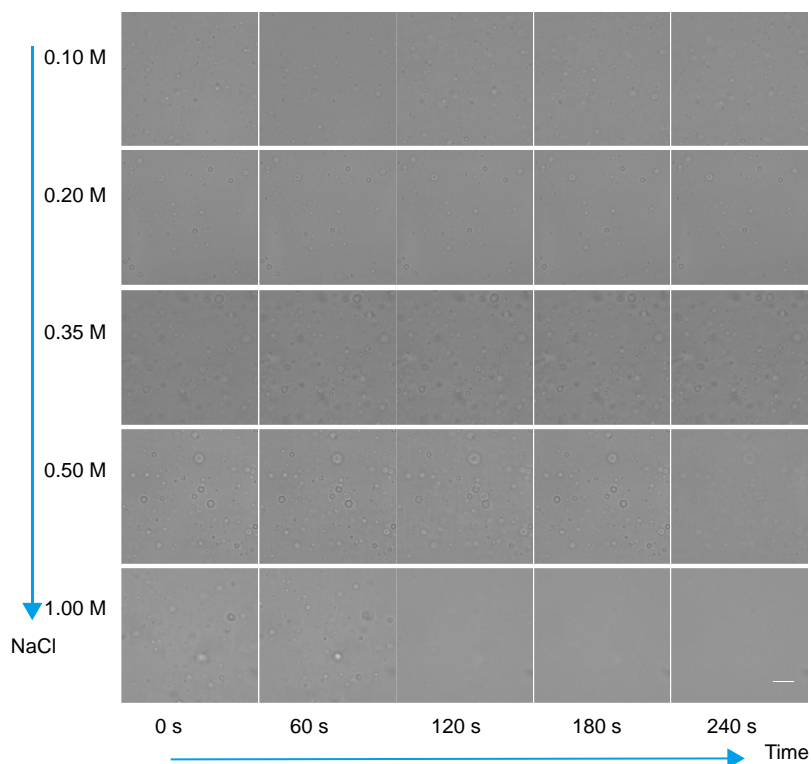


Figure S17. Time-dependent optical microscopy images of coacervate-containing alginate- Ca^{2+} hydrogels after addition of different amounts of NaCl (0.1, 0.2, 0.35, 0.5, 1.0 M). Scale bar: 10 μm .

References

- [1] A. F. Mason, B. C. Buddingh, D. S. Williams, J. H. Van, *J. Am. Chem. Soc.* **2017**, *139*, 17309.
- [2] M. Zhuang, Y. Zhang, S. Zhou, Y. Zhang, K. Wang, J. Nie, J. Liu, *Chem. Commun.* **2019**, *55*, 13880.
- [3] L. Wan, Q. S. Chen, J. B. Liu, X. H. Yang, J. Huang, L. Li, X. Guo, J. Zhang, K. Wang, *Biomacromolecules* **2016**, *17*, 1543.
- [4] G. Gryniewicz, M. Poenie, R. Y. Tsien, *J. Biol. Chem.* **1985**, *260*, 3440.